Engineering Optimization

ISSN: (Print) (Online) Journal homepage: https://www.tandfonline.com/loi/geno20

Structural optimization scheme for acoustic cloaking structures considering general surfaces

Ji Wan Kim & Gil Ho Yoon

ENGINEERING OPTIMIZATION
2022, VOL. 54, NO. 4, 651–664
https://doi.org/10.1080/0305215X.2021.1890725

Taylor & Francis
Taylor & Francis Group

Structural optimization scheme for acoustic cloaking structures considering general surfaces

Ji Wan Kim and Gil Ho Yoon

Department of Mechanical Engineering, College of Engineering Sciences, Hanyang University, Seoul, South Korea

ABSTRACT
The present study presents the application of a structural optimization scheme for a Double Split Hollow Sphere (DSHS) based acoustic cloaking structure for irregular surfaces. For acoustic wave cloaking, many scientific devices utilizing phase differences have been developed. Considering the irregular surfaces of objects to be concealed, acoustic wave reflections become complex with random phase differences and determinations of the involved geometric parameters of cloaking structures become impractical. To determine the geometric parameters of acoustic cloaking devices with DSHS systematically, the present study applies a structural optimization scheme. The present scheme computes and minimizes the differences between the acoustic pressures reflected from irregular surfaces and the reference acoustic pressures without irregular surfaces by optimizing the location and geometric parameters of the DSHS. To show the validity of the present scheme, structural optimization problems are solved for several three-dimensional problems with complex and irregular surfaces.

ARTICLE HISTORY
Received 11 May 2020
Accepted 11 February 2021

KEYWORDS
Acoustic metasurface; double split hollow sphere; acoustic cloaking; phase shift curve

1. Introduction

The present study develops a new structural optimization scheme for acoustic cloaking structures with Double Split Hollow Sphere (DSHS) unit cells for irregular rough surfaces. Much relevant and remarkable research has been presented for scientific and engineering applications of metamaterials and metasurfaces to overcome the limitations of materials and structures found in nature (Shelby, Smith, and Schultz 2001; Schurig *et al.* 2006; Cummer and Schurig 2007; Lu *et al.* 2007; D'Aguanno *et al.* 2012; Liang and Li 2012; Ma *et al.* 2014; Mei and Wu 2014; Tang *et al.* 2014; Zigoneanu, Popa, and Cummer 2014; Ding *et al.* 2015a, 2015b; Esfahlani *et al.* 2016; Song *et al.* 2016; Wang, Chan, and Luk 2016; Zhai *et al.* 2016; Dubois *et al.* 2017). Among many promising applications, the development of cloaking devices—restoring electromagnetic or acoustic waves as if nothing were there and hiding target objects from waves—can be listed as one of the promising applications. The metasurface also can be utilized for the cloaking effect restoring waves from irregular surfaces or uneven terrains. To the best knowledge of the present authors, however, previous studies were limited to simple geometries such as spheres, ellipsoids or flat surfaces by applying theoretical equations for the relationship between the phase difference and the geometry. Note that, with theoretical wave equations, some repeated tasks have to be carried out in order to devise cloaking devices for complex geometries. It is difficult, but important, to keep abreast of theoretical prediction and computational development. With complex geometries, it may be impossible to discover the distributions of metamaterials or the configurations of metasurfaces. To overcome these difficulties, this research presents

CONTACT Gil Ho Yoon gilho.yoon@gmail.com

a structural optimization scheme for determining the optimal parameters of the metamaterials for the cloaking effect. The objective function is set to minimize the difference between the reference pressure and the computed pressure with the configurations of the DSHS unit cells as the design variables.

Countless studies and research on electromagnetic metamaterials and their extension to acoustic metasurface applications have been presented at remarkable pace. Bulk metamaterials have been researched to control electromagnetics with negative refraction (Pendry 2000; Shelby, Smith, and Schultz 2001; Fang *et al.* 2005; Schurig *et al.* 2006; Thomas *et al.* 2011). Practical realization of electromagnetic cloaking has been researched and proposed by Schurig *et al.* (2006). Experimental verification of a negative index of reflection at microwave frequencies was conducted by Shelby, Smith, and Schultz (2001). A superlens allowing the recovery of evanescent waves in an image through surface plasmon excitation was proposed by Fang *et al.* (2005). The lens operating at the frequency of visible light was realized with a thin slab of silver (Pendry 2000). Experimental evidence of rotational Doppler broadening in photoelectron spectra showed good agreement with their theoretical studies (Thomas *et al.* 2011). A metamaterial simultaneously possessing a negative bulk modulus and negative mass density was reported by Ding *et al.* (2007). Light beams providing great flexibility by phase discontinuities was researched by Yu *et al.* (2011). Optical elements introducing an additional spatially non-uniform phase in the incoming waves was researched by Ni *et al.* (2012). An ultrathin directional carpet cloak operating in the reflection geometry based on a generalized Snell's law was proposed by Zhang *et al.* (2013). Using genetic algorithms, labyrinthine metastructures absorbing broadband acoustics were optimized by Kan *et al.* (2015). Some relevant research regarding the optimization of acoustic cloaking devices can be found in Lu *et al.* (2018) and Yu *et al.* (2018). Acoustic cloaking devices with Bézier scatterers were optimized with genetic algorithms by Lu *et al.* (2018). Concentric multi-layered cloaking was proposed by Yu *et al.* (2018). Electromagnetic cloaking devices were optimized by Deng, Liu, and Uhlmann (2017). In addition to wavefront manipulation, the functionality of these surfaces can be extended to metasurface carpet cloaking (Zhang *et al.* 2013; Estakhri and Alù 2014; Ni *et al.* 2015; Orazbayev *et al.* 2015). As metamaterial structures relying on resonance have narrow frequency ranges, one of the challenging topics is to broaden the working frequency (Kan *et al.* 2015). In order to address this issue, several metamaterials with different resonance frequencies can be incorporated. The theories and ideas relating to electromagnetic metamaterials and metasurfaces can also be applied to acoustic applications.

Recently, the concept of acoustic metamaterials and metasurfaces has been proposed for manipulating the reflected or transmitted wavefronts of impinging acoustic waves. Transmission of an incident acoustic wave through a one-dimensional acoustic grating was improved by Lu *et al.* (2007). A DSHS acoustic metamaterial having a transmission dip and accompanied phase advance near the resonant frequency was researched by Ding *et al.* (2013). The concept design of a new class of acoustic metamaterial structure based on a combined heterogeneous DSHS was presented by Choi and Yoon (2018). The controlling of acoustic waves based on ultrathin planar acoustic metasurfaces following a generalized Snell's law was demonstrated by Li *et al.* (2013). The analytical design and experimental realization of acoustic metasurfaces with manipulation of the reflected waves were reported by Li *et al.* (2014). Transmitted wave control and strong reflection with surface mode excitation were researched by Mei and Wu (2014). See also the relevant references for the application of acoustic matching, unidirectional transmission, absorbtion and cloaking in Cummer and Schurig (2007), D'Aguanno *et al.* (2012), Dubois *et al.* (2017), Esfahlani *et al.* (2016), Liang and Li (2012), Ma *et al.* (2014), Song *et al.* (2016), Tang *et al.* (2014), Zhai *et al.* (2016), Zigoneanu, Popa, and Cummer (2014) and Zhu *et al.* (2015a, 2015b). An acoustic metasurface model consisting of split hollow sphere resonator arrays with the property of negative modulus was proposed by Ding *et al.* (2015a). An acoustic metasurface model composed of DSHS resonator arrays with modulated reflected wavefronts was proposed by Ding *et al.* (2015b, 2016). An ultrathin cloak made of acoustic surface impedance leading to acoustic wave invisibility was researched by Chen *et al.* (2011). An acoustic metasurface cloaking for a finite range of frequencies was researched by Farhat *et al.* (2012). Acoustic carpet cloaking by using a metasurface made of graded Helmholtz resonators was experimentally demonstrated by Faure *et al.* (2016). In addition, it is expected that important developments of novel acoustic metasurfaces will be presented in forthcoming years.

To hide an object from incoming electromagnetic, elastic or acoustic waves, the concepts of cloaking devices have been introduced. First of all, so-called carpet cloaks have been of interest and researched by Schurig *et al.* (2006), Cummer and Schurig (2007), Dubois *et al.* (2017), Esfahlani *et al.* (2016), Liang and Li (2012), Ma *et al.* (2014), Song *et al.* (2016), Tang *et al.* (2014), Wang, Chan, and Luk (2016), Zhai *et al.* (2016), Mei and Wu (2014), Zigoneanu, Popa, and Cummer (2014) and Zhu *et al.* (2015a). Surfaces with different impedances along their tangent lines reflect waves randomly and the metasurface technique aims to restore waves reflected from flat surfaces. Normally, man-made layers are added in order to create phase shifting of the reflected waves. State-of-the-art technology utilizes the phase gradient along surfaces to control the reflected or transmitted wavefront. As a result, it is possible to tune the travelling length of the wave and correct the reflected wave. One of the limitations of existing metasurfaces or metamaterials lies in the fact that they exhibit their best performance at a single frequency or at several discrete frequencies. Indeed, it is still an important issue to broaden their working frequencies with a single structure.

This study presents and solves structural optimization problems (size optimization) in order to discover optimal configurations for metamaterials or metasurfaces. The unit cell is set to the DSHS structure and the locations and configurations of the DSHS cells are mainly numerically optimized through Sequential Quadratic Programming (SQP). The DSHS structures are located above the plane or object of interest. For a simple flat plane or object, it is possible to determine the location of the DSHS structure whose frequency is tuned to that of the incoming acoustic wave. In the relevant research, the phase change or shift of the reflected acoustic wave passing through the DSHS structure is incorporated in order to realize cloaking. For flat or segmented surfaces, the geometric configuration of the DSHS structure can be determined through the relationship between the phase shift and the location of the DSHS unit cell. However, for random or smooth surfaces, it can be difficult to realize a cloaking device using the phase shift relationship; the representative distance is hard to determine. To overcome this difficulty in the determination of the geometric parameters of the DSHS structure, they are set as the design variables in the optimization problem minimizing the pressure difference between the reference pressure and the pressure of the current design. To minimize the objective function, its sensitivity values with respect to the design variables are computed. Then the optimization algorithm carries out some finite element simulations and iterations in order to determine optimal values of the geometric parameters of the DSHS structure.

The outline of the present paper is as follows: theories of metasurface structure and the optimization formulation are described in Section 2. To illustrate the DSHS structure of the cloaking device and extraordinary acoustic reflection, the offset distances between the surface of interest and the DSHS structure are determined manually. Then the difficulties and limitations of the manual determination for complex surfaces are discussed and the optimization formulation is presented. In Section 3, several optimization examples are solved in order to show the effectiveness of the present optimization formulation for the cloaking device. Finally, some concluding remarks are made in Section 4.

2. Model and method

2.1. Theory of DSHS-based metamaterials

This research presents a structural optimization scheme determining the location and geometric parameters of DSHS-based metamaterials (Ding *et al.* 2013, 2015a, 2015b, 2016; Choi and Yoon 2018). Some relevant research on cloaking devices and metamaterials has mainly been targeted on acoustic or electromagnetic waves reflected from flat surfaces or simple objects (Schurig *et al.* 2006; Estakhri and Alù 2014; Ding *et al.* 2015a, 2015b, 2016; Esfahlani *et al.* 2016; Faure *et al.* 2016; Dubois *et al.* 2017). Using an analytical formulation for the phase difference induced by metamaterials, the optimal parameters—*i.e.* location, shape and material properties—can be determined (Schurig *et* *al.* 2006). For some random and stochastic surfaces, to the present authors' best knowledge, it is not easy to realize the cloaking phenomenon owing to difficulties in determining representative geometric parameters. For the extension of cloaking devices to relatively complex subjects or surfaces, the issues with choosing the optimal parameters for cloaking devices should be addressed.

For the sake illustrating DSHS-based metamaterials, Figure 1(a) shows a unit structure of the DSHS acoustic metamaterial above a flat plate and the phase shift curve computed by finite element simulation. The acoustic resonance frequency of the DSHS structure is tuned to the frequency of the incoming wave, in this case 1700 Hz. Utilizing the phase shift of the wave, cloaking of the surface can be achievable (Faure *et al.* 2016). The values of the phase shift make it possible to determine the geometric parameters of the unit cell and realize the cloaking. In other words, by posing one unit cell or multiple unit cells as a metasurface above a rough surface, extraordinary wave reflection can be realized.

First of all, the following theoretical equation (1) can be employed as a generalized Snell's law derived from Fermat's principle:

$$n_i k(\sin\theta_r - \sin\theta_i) = \xi, \quad \xi = \frac{\mathrm{d}\Phi}{\mathrm{d}x}, \tag{1}$$

where θ_i and θ_r denote the angles of the incident wave and the reflected wave, respectively. The refractive index of the medium is denoted by n_i. The phase shift gradient, $\mathrm{d}\Phi/\mathrm{d}x$, is set to a non-zero constant. The generalized Snell's law can be reformulated as follows:

$$\sin\theta_r - \sin\theta_i = \frac{\mathrm{d}\Phi}{\mathrm{d}x}\frac{1}{n_i k}. \tag{2}$$

In the case of air, the following condition can be imposed:

$$n_i = n_{\mathrm{air}} \approx 1, \quad k = \frac{2\pi}{\lambda}, \tag{3}$$

where the wave vector and the wavelength are denoted by k and λ. The reflection angle can be simplified as follows:

$$\theta_r = \arcsin\left(\sin(\theta_i) + \frac{\lambda}{2\pi}\frac{\mathrm{d}\Phi}{\mathrm{d}x}\right). \tag{4}$$

Assuming that the acoustic wave propagates normal to the surface, the following equation can be derived and used to correlate the extended length $\triangle L$ and the difference of the phase shift $\triangle\Phi$:

$$\triangle\Phi(x) = -2k\triangle L. \tag{5}$$

Consider the structure in Figure 1(b)(left and right) with the DSHS structure with the phase shift curve in Figure 1(a) tuned to 1700 Hz. The dimensions of the DSHS structure are set to make the resonance frequency of the DSHS structure 1700 Hz ($d = 3.1$ mm, $R = 0.0125$ m, thickness = 0.5 mm, $c = 343$ m/s, $S = 4(d/2)^2\pi$, $V = 4/3\pi(R)^3$, and the first resonance frequency of DSHS = $c\sqrt{2S/V(\mathrm{thickness})}/2\pi$). Figure 1(b), left, shows a simulation with length L and its reflected acoustic wave p_r as a reference: $p_r = p - p_i$, where the total acoustic pressure, the reflected acoustic pressure and the incident acoustic pressure are denoted by p, p_r and p_i, respectively. Figure 1(b), right, shows the extended domain ($L_{\mathrm{extended}} = 0.255$ m) and the reflected acoustic wave. Due to the change of the analysis domain, the acoustic waves of Figure 1(b), left and right, are different from each other. To compensate for this difference, it is possible to locate the DSHS structure above the flat bottom surface as shown in Figure 1(c). To determine the location (the offset distance from the bottom surface) of the DSHS structure, the phase shift curve in Figure 1(a) needs to be considered. As the phase difference calculated by (5) is about −0.9342 rad, the corresponding geometric values read in Figure 1(a) are

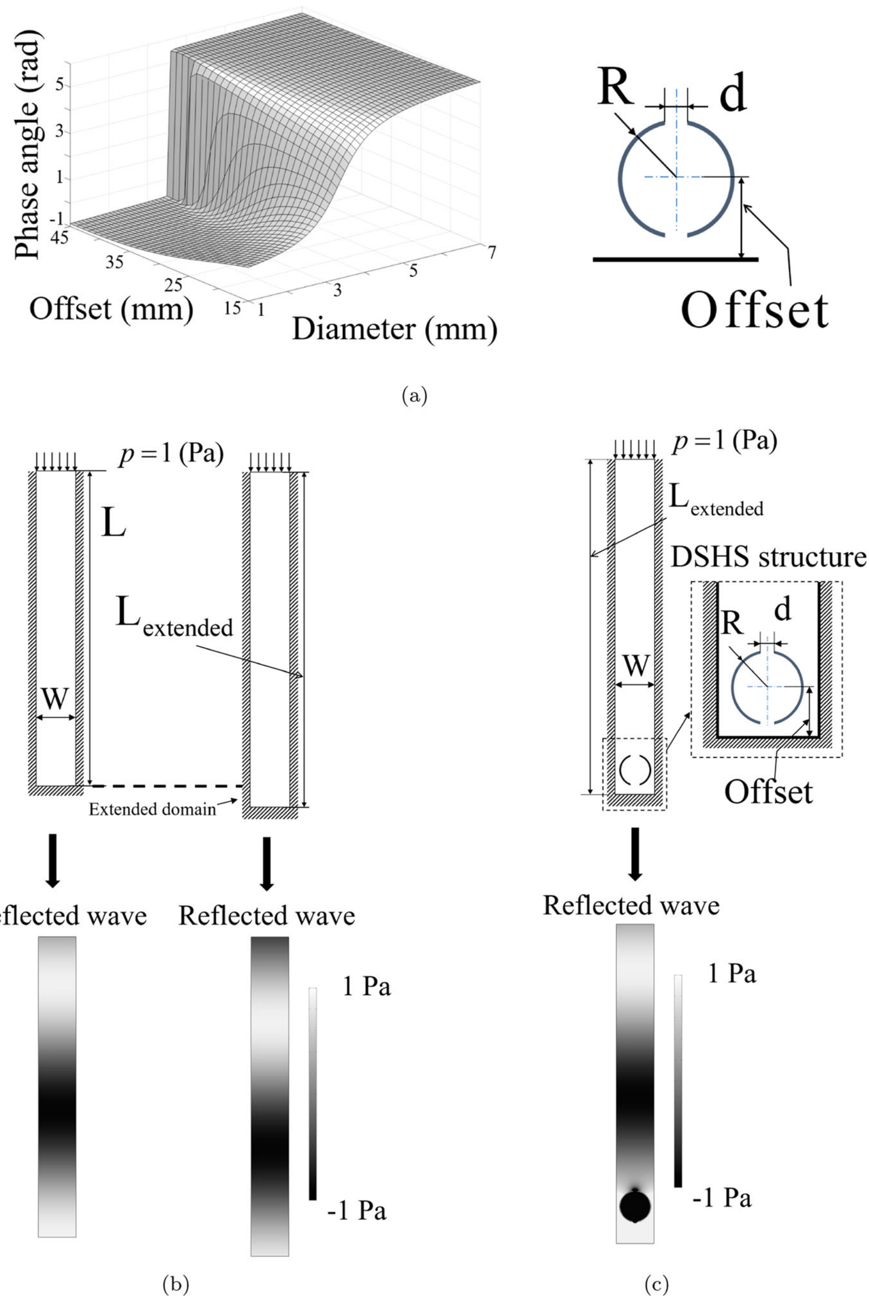

Figure 1. Manual determination of the geometric parameters for the DSHS cloaking device (media: air, density = 1.25 kg/m^3, wavespeed = 343 m/s, acoustic frequency = 1700 Hz, $L = 0.24$ m, $L_{\text{extended}} = 0.255$ m, $W = 0.03$ m, Offset = 0.03 m, d = 3.1 mm, R = 12.5 mm, thickness = 0.5 mm). (a) Phase shift by DSHS; (b) reflected acoustic waves without (left) and with (right) the disturbance; and (c) corrected reflected acoustic wave with DSHS metastructure. (Note that the reflected wave in (c) is similar to the reflected acoustic wave (left) in (a).)

30 mm for the offset value and 3.1 mm for the diameter. Thus, the DSHS structure with the geometric parameters is installed in Figure 1(c). As illustrated, the acoustic pressure is modified such that the reflected acoustic wave is similar to the reflected acoustic wave in Figure 1(b), left. This approach and similar approaches have been applied in many cloaking devices (Li *et al.* 2014; Ding *et al.* 2016; Faure

et al. 2016; Choi and Yoon 2018). This research does adopt this idea but employs the optimization algorithm in order to determine the geometric parameters for complex surfaces.

2.2. Optimization formulation

The determination of the locations and shapes of the DSHS structures for the cloaking of arbitrary manifold reflection surfaces can be difficult. To address and overcome this issue, a structural optimization scheme is proposed. As illustrated in the previous subsection, some relevant research has determined the geometric parameters of the metamaterials using the phase shift curve manually (Ding *et al.* 2016; Faure *et al.* 2016).

Such approaches are applicable when the reflection surface is smooth enough with few design variables. When the reflection surface becomes rough, the scattering of the acoustic wave from the surface makes it difficult to determine the geometric parameters. In addition, the determination of the parameters becomes more difficult with an increased number of design variables, which are the geometric parameters of the metamaterials. In order to address these issues effectively, a structural optimization scheme with the geometric parameters as the design variables in (6) can be employed. The norm of the difference between the acoustic pressure $\mathbf{P}$ and the reference acoustic pressure $\mathbf{P}_{\text{ref}}$ is set as the objective function as shown in Figure 2. The reference acoustic pressure here can be set as the acoustic pressure without any geometric perturbation:

$$\begin{aligned} &\underset{\mathbf{X}}{\text{Minimize}} \quad \int_{\Omega} \|\mathbf{P}-\mathbf{P}_{\text{ref}}\|^2 \, \mathrm{d}\Omega \approx \sum \|\mathbf{P}-\mathbf{P}_{\text{ref}}\|^2 \\ &\mathbf{X} = [X_1, X_2, \ldots, X_N] \\ &X_i^{\text{lower}} \leqslant X_i \leqslant X_i^{\text{upper}}, \end{aligned} \tag{6}$$

where the objective domain is defined at Ω and the design variables are denoted by $\mathbf{X}$. The number of design variables is denoted by N. The upper and lower bounds of the ith design variables are set as X_i^{lower} and X_i^{upper}, respectively. In order to evaluate the objective function, the difference norms of the reference response $\mathbf{P}_{\text{ref}}$ and the computed pressure $\mathbf{P}$ are evaluated at evenly distributed points in the objective domain. The choice of the objective domain also affects the optimization result. With a small domain for Ω, it may be difficult to determine the optimal design variables modifying the reflected acoustic wave as if there were no object. In optimization examples in this article, the domain Ω is chosen to cover the fraction of the analysis domain whose length is comparable with the wavelength of the incoming wave. In real engineering applications, acoustic damping such as porous materials,

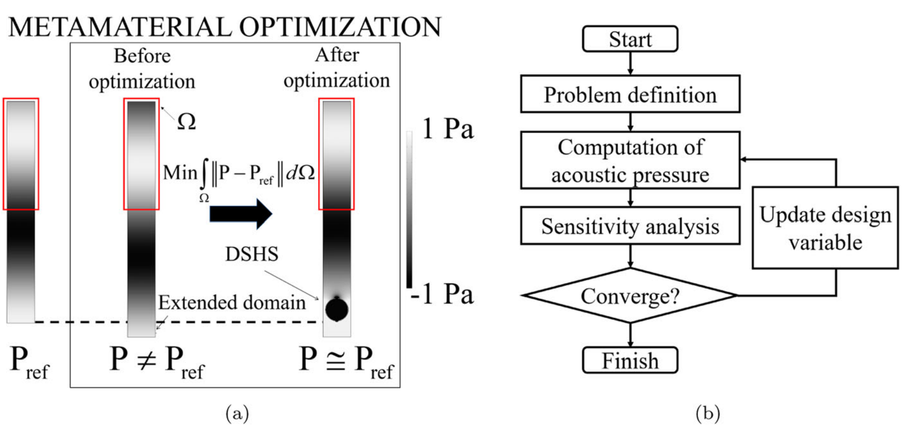

Figure 2. The optimization formulation: (a) the definition of the objective function; and (b) the optimization process.

thermal dissipation, viscosity dissipation and nonlinear materials may affect the wave propagation. In the present study, the effect of acoustic damping is ignored. The present local optimization algorithm uses a first-order approximation with the function value and its gradient values with respect to the design variables, and the optimized locations of the DSHS structures are the local optima. The designs are the local optima from an optimization point of view. Alternative algorithms can be used to obtain several global solutions. For example, genetic or similar algorithms can be employed. However, they often require a substantial increase of computation time.

3. Applications

To show the application of the optimization process of the DSHS acoustic cloaking device, this section provides several optimization examples of acoustic cloaking devices for irregular surfaces. Several three-dimensional straight and curved surfaces with varying impedance are considered; corrections or adjustments of their impedance mismatches are difficult to achieve either manually or theoretically. This research suggests applying the structural optimization scheme in (6) to modify acoustic impedance mismatches in reflected acoustic waves. The finite difference method is employed to compute the sensitivity value and the SQP algorithm in MATLAB® is used to solve the above optimization problem. As the optimization procedure is carried out with the finite difference method, the optimization procedure takes a long time in the case of multiple metamaterial units. To address this, it is possible to use parallel computation to accelerate the computation process of the sensitivity values.

With these different height profiles of reflection surfaces, strong acoustic impedance variations in the reflected acoustic waves are observed. With the present DSHS metasurfaces, the phase shifts caused by surfaces with random heights are adjusted in order to obtain a reflected wave as if the surfaces were flat. Compared with the relevant research (Cummer and Schurig 2007; Esfahlani *et al.* 2016; Faure *et al.* 2016; Zhai *et al.* 2016), the present DSHS cloaking metasurface has the merit of the easy installation without modification of the surfaces themselves. In addition, to the present authors' best knowledge, the application of DSHS for surface cloaking has never been tried before.

3.1. Example 1: optimization of cloaking structure on a flat surface

For the first optimization example, Figure 3 considers the optimization example of Figure 1 with the structural optimization algorithm; although the illustration is two-dimensional, the simulations and optimizations are carried out in a three-dimensional domain. Note that the basic dimensions of the DSHS structures are set to make the first resonance frequency of the DSHS structure 1700 Hz. In order to evaluate the objective function, the norms of the difference between the target reflected acoustic response and the reflected pressure computed with a given design is evaluated at 20 by 20 evenly distributed points; the points of the other examples are chosen in the same manner and with a negligible effect on the optimization results with another set of points sufficiently representing the acoustic wave. The x- and z-coordinates of the points are chosen as follows:

$$\begin{aligned} x_p &= [0 : \Delta x : W](\Delta x = W/n,\ n = 20) \\ z_p &= [0 : \Delta z : L_{\text{objective}}](\Delta z = L_{\text{objective}}/n,\ n = 20). \end{aligned} \tag{7}$$

Although the offset value, *i.e.* 30 mm, can be manually determined by the analytical equation, this example is devised to show that the present optimization algorithm can find the manually optimized result, 30 mm, of Figure 1. For an optimization test, the initial offset value is set to 45 mm. After seven iterations of the present optimization scheme, the final optimized offset value, 29.9656 mm, can be obtained. Considering the human factor in determining the offset value, this value, 29.9656 mm, is fairly accurate and accurate enough to correct the reflected acoustic wave. From an optimization theory point of view, a non-convex optimization problem with several local optima is expected for the acoustic optimization problem. However, in this particular example with one DSHS structure,

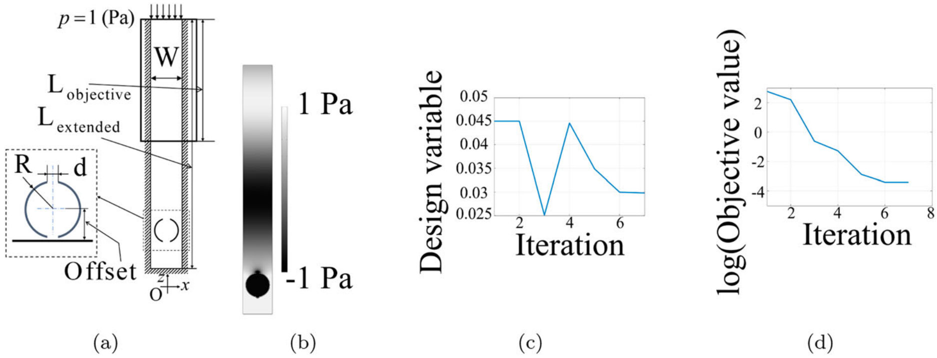

Figure 3. Optimization of DSHS with the incoming wave (1700 Hz): (a) the geometric parameter of the optimization condition in Figure 1 (air, $W = 30$ mm, $L = 255$ mm, $L_{objective} = 120$ mm, $R = 12.5$ mm, $d = 3.1$ mm, centre aligned horizontally, initialoffset = 45 mm, 25 mm ≤ offset ≤ 55 mm); (b) the optimization result for a single DSHS on a plane surface ($\text{offset}_{optimized} =$ 29.9656 mm); (c) the evolution of the design parameter; and (d) the optimization history—$f_{optimized} = 0.3964\ (N/m^2)^2$, $f_{void} = 5.7414 \times 10^5\ (N/m^2)^2$.

the optimization problem becomes convex and the value can be obtained without the local optimum issue. The optimization history and the evolution of the design parameter can be found in Figure 3(c,d). The present algorithm can also be applied to another frequency case (not presented here).

Figure 4 solves the examples determining the optimized offset values for the three DSHS structures inside a wide channel with a 1700 Hz incoming wave. Figure 4(a) shows the problem definition and Figure 4(b) shows the reflected acoustic wave with the same 30 mm offset values as the three DSHSs. As the domain of this problem is just an extended domain of that in Figure 3, the offset values of the DSHSs are set at 30 mm in Figure 4(b). The acoustic wave locally reflects around the DSHS structures increasing the complexity. To investigate the convexity of the optimization problem, the different initial offset values are tested in Figure 4(c–e). The different optimized offset values can be obtained, which proves that the optimization problem is non-convex. By comparing the objective values, it turns out that the optimized objectives (objectivevalues $= 0.0172 (N/m^2)^2$, 0.000,5699 $(N/m^2)^2$ and 0.000,6348 $(N/m^2)^2$) with the present scheme are better than the design (objectivevalue $= 0.3601 (N/m^2)^2$) with 30 mm for the offset value in terms of the objective function. Figure 4(f) shows the responses along the centreline. From an optimization point of view, this implies that the present optimization formulation has several local optima, unlike the optimization problem with one design variable in Figure 3. As the metamaterials relying on the resonance have a narrow frequency range, it is one of the challenging topics to broaden the working frequency. To address this, it is possible to use multiple metamaterials with different working frequencies.

3.2. Example 2: optimization of cloaking structure on inclined surfaces

For the 1700 Hz incident acoustic wave, Figure 5 shows optimization examples for surfaces inclined at 10°, 20° and 26.5651°; the angle 26.5651° is chosen considering the geometric constraint. To compensate for the effect of the inclined surfaces on the reflected acoustic wave, three DSHS structures with resonance frequencies 1700 Hz are installed above the inclined surfaces. Note that, due to the inclined surfaces, the reflected acoustic waves become more random compared with those from a flat surface and would not be accurate to apply the manual approach with Equation (5) to determine the offset values of the DSHS unit structures. Theoretically, as the distance between the inclined surface and the surface of the input pressure is continuously changing, it is difficult to determine the offset distances of the DSHS structures. Figure 5(b) shows the optimized layout for $\theta = 10°$ and its reflected acoustic wave. With 95 mm for the initial offset values, it is possible to obtain $\text{Offset}_1 = 64.9634$ mm, $\text{Offset}_2 = 66.7263$ mm and $\text{Offset}_3 = 45.1811$ mm. Figure 5(c) shows the

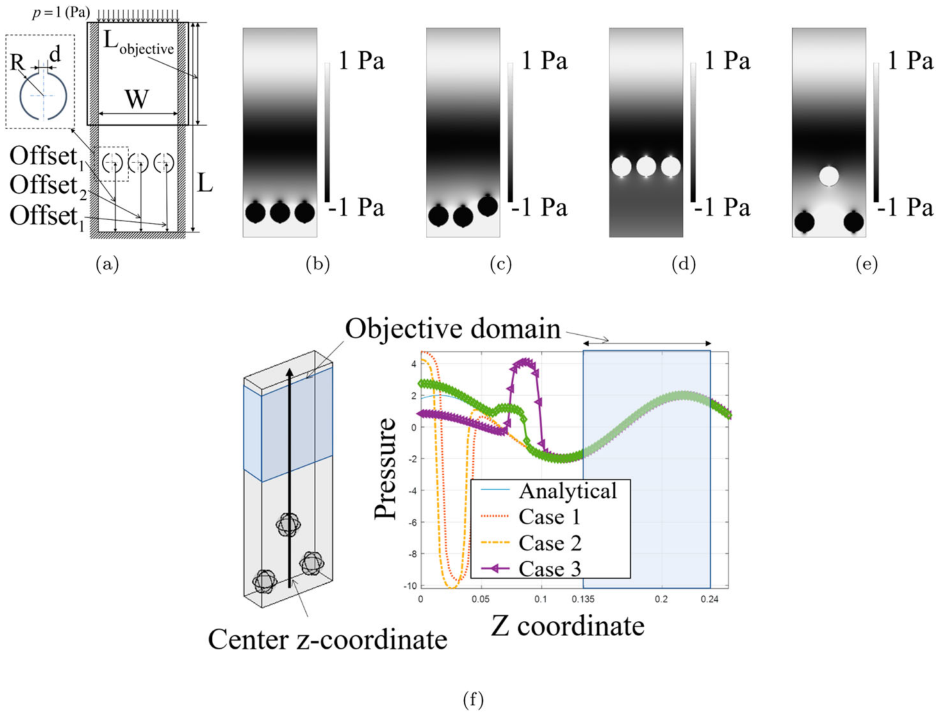

Figure 4. An optimization example with three DSHS-based metasurfaces inside a channel: (a) problem definition (air, $W = 90$ mm, $L = 255$ mm, $L_{\text{objective}} = 120$ mm, $d = 3.1$ mm, $R = 12.5$ mm, thickness of DSHS $= 0.5$ mm, x-coordinates of the DSHSs are 15, 45 and 75 mm); (b) the analysis with the three DSHS structures (manualoffset $= 30$ mm, objectivefunction $= 0.3601\ (\text{N/m}^2)^2$); (c) Case 1: the optimization result ($\text{Offset}_1 = 26.0188$ mm, $\text{Offset}_2 = 25.0336$ mm, $\text{Offset}_3 = 38.0011$ mm) with the initial distribution ($\text{Offset}_{1,2,3}^{\text{initial}} = 35$ mm, 25 mm $\leq \text{Offset}_{1,2,3} \leq$ 40 mm, objectivefunction $= 0.0172\ (\text{N/m}^2)^2$); (d) Case 2: the optimization result ($\text{Offset}_1 = 85.8990$ mm, $\text{Offset}_2 = 86.1719$ mm, $\text{Offset}_3 = 85.9427$ mm) with the initial distribution (evenly distributed horizontally, $\text{Offset}_{1,2,3}^{\text{initial}} = 95$ mm, 16 mm $\leq \text{Offset}_{1,2,3} \leq$ 115 mm, objectivefunction $= 0.000,5699\ (\text{N/m}^2)^2$); (e) Case 3: the optimization result ($\text{Offset}_1 = 18.5506$ mm, $\text{Offset}_2 = 74.2574$ mm, $\text{Offset}_3 = 18.6415$ mm) with the initial distribution ($\text{Offset}_{1,2,3}^{\text{initial}} = 55$ mm, 16 mm $\leq \text{Offset}_{1,2,3} \leq$ 115 mm, objectivefunction $= 0.000,6348\ (\text{N/m}^2)^2$); and (f) comparison of the pressure distributions.

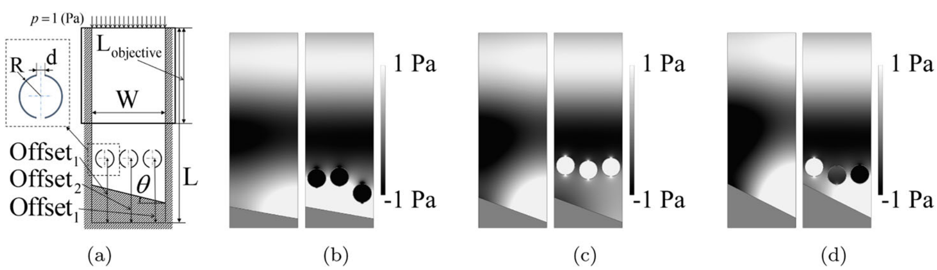

Figure 5. Optimization results for the different slopes: (a) problem definition (air, $W = 90$ mm, $L = 255$ mm, $L_{\text{objective}} = 120$ mm, $d = 3.1$ mm, $R = 12.5$ mm, thickness of DSHS $= 0.5$ mm, x-coordinates of the DSHSs are 15, 45 and 75 mm); (b) an optimum design with $\theta = 10^\circ$ ($\text{Offset}_1 = 64.9634$, $\text{Offset}_2 = 66.7263$, $\text{Offset}_3 = 45.1811$ mm) with the initial distribution ($\text{Offset}_{1,2,3}^{\text{initial}} =$ 95 mm, 38 mm $\leq \text{Offset}_1 \leq$ 115 mm, 33 mm $\leq \text{Offset}_2 \leq$ 115 mm, 28 mm $\leq \text{Offset}_3 \leq$ 115 mm); (c) an optimum design with $\theta = 20^\circ$ ($\text{Offset}_1 = 81.3220$, $\text{Offset}_2 = 75.6013$, $\text{Offset}_3 = 79.3568$ mm) with the initial distribution ($\text{Offset}_{1,2,3}^{\text{initial}} = 95$ mm, 48 mm $\leq \text{Offset}_1 \leq$ 115 mm, 37 mm $\leq \text{Offset}_2 \leq$ 115 mm, 26 mm $\leq \text{Offset}_3 \leq$ 115 mm); and (d) an optimum design with $\theta = 26.5651^\circ$ ($\text{Offset}_1 = 79.2431$, $\text{Offset}_2 = 68.8249$, $\text{Offset}_3 = 70.0518$ mm) with the initial distribution ($\text{Offset}_{1,2,3}^{\text{initial}} = 95$ mm, 70 mm $\leq \text{Offset}_1 \leq$ 115 mm, 55 mm $\leq \text{Offset}_2 \leq$ 115 mm, 40 mm $\leq \text{Offset}_3 \leq$ 115 mm).

optimized layout for $\theta = 20^\circ$ and its reflected acoustic wave. With 95 mm for the initial offset values, it is possible to obtain $\text{Offset}_1 = 81.3220$ mm, $\text{Offset}_2 = 75.6013$ mm and $\text{Offset}_3 = 79.3568$ mm. Comparing the offset values in Figure 5(b), the DSHS structures move up. Figure 5(d) shows the optimized layout for $\theta = 26.5651^\circ$. With 95 mm for the initial offset values, it is possible to obtain $\text{Offset}_1 = 79.2431$ mm, $\text{Offset}_2 = 68.8249$ mm and $\text{Offset}_3 = 70.0518$ mm. Note that, regardless of the inclination angle, the reflected acoustic waves become similar to those for a flat surface. This example shows the validity and potential of the present optimization scheme for metamaterials.

3.3. Example 3: optimization of cloaking structures on irregular surfaces

Figure 6(a) shows an optimization example of an irregular surface with three DSHS units and the reference pressure. Rather than a flat surface, an arbitrarily chosen curved surface is constructed at

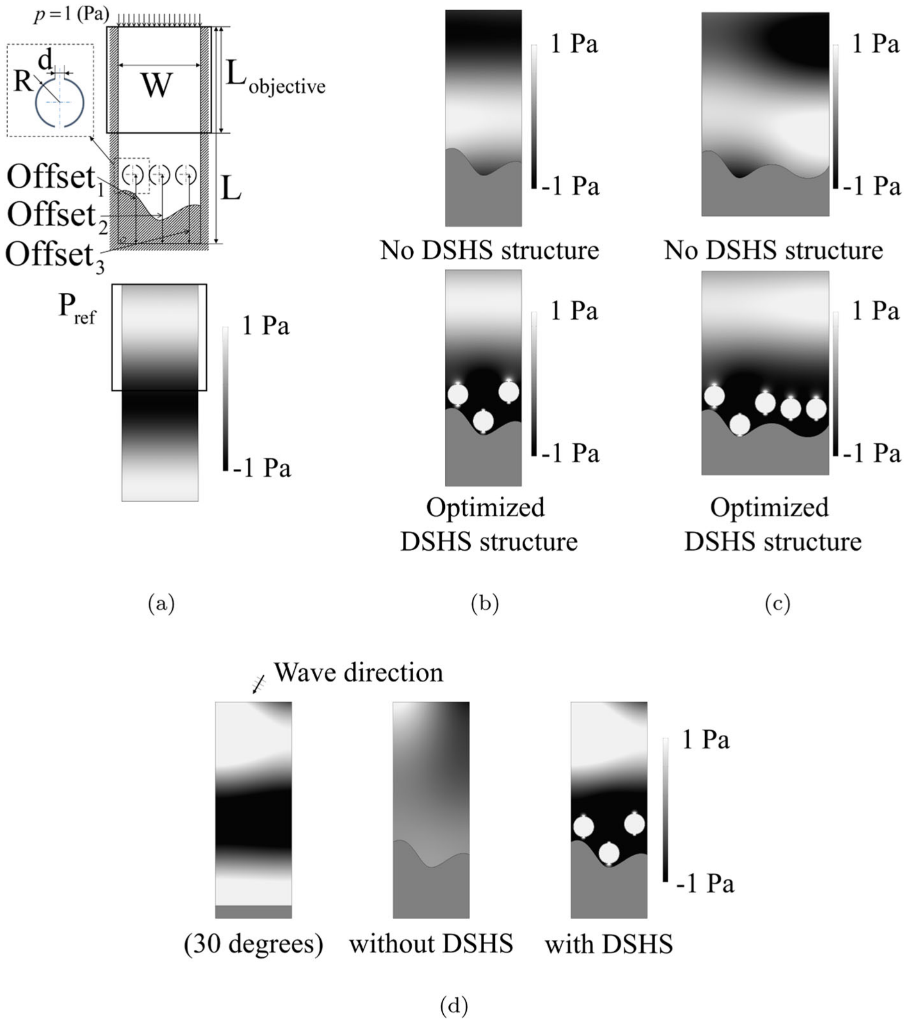

Figure 6. Optimization problem with an irregular surface: (a) problem definition ($R = 12.5$ mm, $d = 3.1$ mm, thickness = 0.5 mm, $L = 255$ mm, $W = 90$ mm, x-coordinates of the DSHSs are 15, 45 and 75 mm, $L_{\text{objective}} = 120$ mm, $\mathbf{Pos}_{\text{interpolation}}$ = [(0, 0.09), (0.015, 0.09), (0.045, 0.06), (0.075, 0.075), (0.09, 0.075)] mm); (b) the reflected pressure without and with the three optimized DSHS structures; (c) the reflected pressure without and with the five optimized DSHS structures; and (d) the oblique acoustic propagation test.

the bottom of the surface. The surface projected through thickness is defined by interpolating the five points $\mathbf{Pos}_{\text{interpolation}}$ in Figure 6. The reference pressure in Figure 6(a), bottom, is computed without the interpolated surface. Nevertheless, the curved surface causes complex wave propagation as shown in Figure 6(b), top, and the determination of the optimized locations of the DSHS structures becomes more difficult. To the present authors' knowledge, this kind of complex geometry has not been considered before this research. As illustrated, the pressure of the optimized configuration (Figure 6(b), bottom) shows good agreement with the reference pressure (Figure 6(a), bottom). In addition, the present DSHS structure can be used to cloak random surfaces without modifying the surfaces themselves. To show the example with an enlarged domain, Figure 6(c) presents the optimization problem with an enlarged irregular surface and five DSHS units. The horizontal size of the analysis domain is 0.15 m, or approximately 0.75 times the wavelength. As illustrated in Figure 6(c), the present optimization process works for this enlarged domain.

Acoustic propagation in the y-direction is only considered for analysis and optimization, and it is recommended to check whether the current metamaterial designs are valid for oblique wave propagation. Note that the acoustic wave propagation in the x- and y-directions can be decomposed. Thus, it turns out that the present designs work for oblique wave propagation too. For an example, Figure 6(d) shows the reanalysed acoustic wave propagation. As shown, the present designs work for oblique acoustic wave propagation. In Figure 6(d), with oblique wave propagation, the wave propagation in the y-direction is cloaked. It is worth noticing that relevant research optimizes acoustic cloaking devices describing their geometry with a Bézier curve and a genetic algorithm (Lu *et al.* 2018). The present work also parameterizes the locations of the sphere and these parameters are optimized using a gradient-based optimization method. The above results prove that it is possible to optimize the locations and geometries of DSHS-based cloaking devices without deriving the analytical phase angle shift. The other geometric parameters of the DSHS structures are manually tuned to set their resonance frequencies to the frequency of the incoming acoustic wave. Additionally, the number of design variables is limited, so reducing the computational effort of optimization. While it is possible to optimize the shape or size of DSHS structures systematically, the structural optimization of these parameters increases manufacturing costs and is not pursued here.

Figure 7 shows another optimization example with the irregular surface defined by

$$z = 0.01 \times \sin\left[\frac{2\pi}{0.06}x - \frac{\pi}{2}\left(\frac{1}{0.015}y + 1\right)\right] + 0.025$$

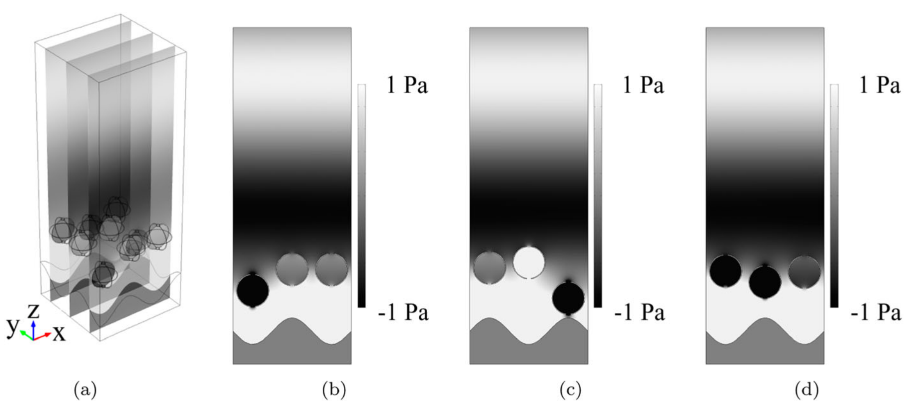

Figure 7. Example with a random surface ($z = 0.01 \times \sin(\frac{2\pi}{0.06}x - \frac{\pi}{2}(\frac{1}{0.015}y + 1)) + 0.025$): (a) optimized offset values ($\text{Offset}_1 = 55.7745$ mm, $\text{Offset}_2 = 71.7798$ mm, $\text{Offset}_3 = 71.6088$ mm, $\text{Offset}_4 = 72.9565$ mm, $\text{Offset}_5 = 77.0368$ mm, $\text{Offset}_6 = 50.0398$ mm, $\text{Offset}_7 = 70.5377$ mm, $\text{Offset}_8 = 62.1797$ mm, $\text{Offset}_9 = 69.6707$ mm, initial design distribution $\text{Offset}_{1-9}^{\text{initial}} = 60$ mm, 50 mm $\leq \text{Offset}_{1\,3} \leq$ 115 mm.); and (b)–(d) the cross sections of the reflected acoustic presssure at (a).

and nine DSHS structures. In this example, note that the defined surface is covered by the nine DSHS structures and, to the present authors' best knowledge, the conventional approach relying on the theoretical formulation bears some limitations in determining the locations of the DSHS structures. The DSHS structures are evenly distributed on the domain and the heights of the nine DSHS structures are optimized. By investigating the acoustic pressure at the cross sections in Figure 7(b–d), it turns out that cloaking devices are obtained. This example proves that the present optimization scheme can determine an optimal configuration of the present metasurface.

4. Conclusions

This research suggests realizing acoustic cloaking devices for irregular surfaces by solving an optimization problem determining the optimal parameters of the DSHS-based acoustic cloaking structures. Owing to irregular surfaces, theoretical derivations of reflected acoustic waves are often limited and it is necessary to rely on numerical analysis and optimization schemes for cloaking devices. Geometric parameters such as height, size or thickness can be set as the design variables; in principle, any geometric parameter can be used as design variables. By minimizing the norm of the difference between the acoustic pressure and the reference acoustic pressure by varying the design variables, it is possible to realize acoustic cloaking devices. In order to show the validity of the present scheme, several three-dimensional problems were solved. In the numerical optimizations in this article, the optimization results are numerically better than those of designs optimized manually. In addition, multiple local optima whose objective values are also better than those of manually determined designs can be obtained. The optimized designs also cloak for oblique acoustic wave propagation. The examples show that the present scheme can search the design space in order to determine several local optima, and acoustic cloaking devices can be designed successfully. For future research, the present scheme can be extended for the optimization of metasurfaces.

Acknowledgments

This work was supported by a National Research Foundation of Korea (NRF) grant funded by the Korea government (MSIT) [NRF-2019R1A2C2084974].

Disclosure statement

No potential conflict of interest was reported by the authors.

Funding

This work was supported by a National Research Foundation of Korea (NRF) grant funded by the Korea government (MSIT) (NRF-2019R1A2C2084974).

References

Chen, Pai-Yen, Mohamed Farhat, Sébastien Guenneau, Stefan Enoch, and Andrea Alù. 2011. "Acoustic Scattering Cancellation Via Ultrathin Pseudo-Surface." *Applied Physics Letters* 99 (19): Article ID 191913. doi:10.1063/1.3655141.

Choi, Jung Sik, and Gil Ho Yoon. 2018. "Acoustic Metamaterials with Combined Heterogeneous Double-Split Hollow Sphere for Noise Reduction." *Journal of Vibration and Control* 24 (21): 4933–4944.

Cummer, Steven A., and David Schurig. 2007. "One Path to Acoustic Cloaking." *New Journal of Physics* 9 (3): Article ID 45.

D'Aguanno, G., K. Q. Le, R. Trimm, Andrea Alù, N. Mattiucci, A. D. Mathias, N. Aközbek, and M. J. Bloemer. 2012. "Broadband Metamaterial for Nonresonant Matching of Acoustic Waves." *Scientific Reports* 2: Article ID 340. doi:10.1038/srep00340.

Deng, Youjun, Hongyu Liu, and Gunther Uhlmann. 2017. "Full and Partial Cloaking in Electromagnetic Scattering." *Archive for Rational Mechanics and Analysis* 223 (1): 265–299.

Ding, Changlin, Huaijun Chen, Shilong Zhai, Song Liu, and Xiaopeng Zhao. 2015a. "The Anomalous Manipulation of Acoustic Waves Based on Planar Metasurface with Split Hollow Sphere." *Journal of Physics D: Applied Physics* 48 (4): Article ID 045303.

Ding, Changlin, Huaijun Chen, Shilong Zhai, and Xiaopeng Zhao. 2013. "Acoustic Metamaterial Based on Multi-Split Hollow Spheres." *Applied Physics A* 112 (3): 533–541.

Ding, Yiqun, Zhengyou Liu, Chunyin Qiu, and Jing Shi. 2007. "Metamaterial with Simultaneously Negative Bulk Modulus and Mass Density." *Physical Review Letters* 99 (9): Article ID 093904.

Ding, Chang-Lin, Zhen-Ru Wang, Fang-Liang Shen, Huai-Jun Chen, Shi-Long Zhai, and Xiao-Peng Zhao. 2016. "Experimental Realization of Acoustic Metasurface with Double-Split Hollow Sphere." *Journal Solid State Communications* 229: 28–31.

Ding, Changlin, Xiaopeng Zhao, Huaijun Chen, Shilong Zhai, and Fangliang Shen. 2015b. "Reflected Wavefronts Modulation with Acoustic Metasurface Based on Double-Split Hollow Sphere." *Applied Physics A* 120 (2): 487–493.

Dubois, Marc, Chengzhi Shi, Yuan Wang, and Xiang Zhang. 2017. "A Thin and Conformal Metasurface for Illusion Acoustics of Rapidly Changing Profiles." *Applied Physics Letters* 110 (15): Article ID 151902.

Esfahlani, Hussein, Sami Karkar, Herve Lissek, and Juan R. Mosig. 2016. "Acoustic Carpet Cloak Based on An Ultrathin Metasurface." *Physical Review B* 94 (1): Article ID 014302.

Estakhri, Nasim Mohammadi, and Andrea Alù. 2014. "Ultra-Thin Unidirectional Carpet Cloak and Wavefront Reconstruction with Graded Metasurfaces." *IEEE Antennas and Letters, Wireless Propagation* 13: 1775–1778.

Fang, Nicholas, Hyesog Lee, Cheng Sun, and Xiang Zhang. 2005. "Sub-Diffraction-Limited Optical Imaging with a Silver Superlens." *Science* 308 (5721): 534–537.

Farhat, Mohamed, Pai-Yen Chen, Sébastien Guenneau, Stefan Enoch, and Andrea Alù. 2012. "Frequency-Selective Surface Acoustic Invisibility for Three-Dimensional Immersed Objects." *Physical Review B* 86 (17): Article ID 174303.

Faure, Cédric, Olivier Richoux, Simon Félix, and Vincent Pagneux. 2016. "Experiments on Metasurface Carpet Cloaking for Audible Acoustics." *Applied Physics Letters* 108 (6): Article ID 064103. doi:10.1063/1.4941810.

Kan, Weiwei, Victor M. García-Chocano, F. Cervera, Bin Liang, Xin-ye Zou, Lei-lei Yin, Jianchun Cheng, and José Sánchez-Dehesa. 2015. "Broadband Acoustic Cloaking Within An Arbitrary Hard Cavity." *Physical Review Applied* 3 (6): Article ID 064019.

Li, Yong, Xue Jiang, Rui-qi Li, Bin Liang, Xin-ye Zou, Lei-lei Yin, and Jian-chun Cheng. 2014. "Experimental Realization of Full Control of Reflected Waves with Subwavelength Acoustic Metasurfaces." *Physical Review Applied* 2 (6): Article ID 064002.

Li, Yong, Bin Liang, Zhong-ming Gu, Xin-ye Zou, and Jian-chun Cheng. 2013. "Reflected Wavefront Manipulation Based on Ultrathin Planar Acoustic Metasurfaces." *Scientific Reports* 3: Article ID 2546. doi:10.1038/srep02546.

Liang, Zixian, and Jensen Li. 2012. "Extreme Acoustic Metamaterial by Coiling Up Space." *Physical Review Letters* 108 (11): Article ID 114301.

Lu, Ming-Hui, Xiao-Kang Liu, Liang Feng, Jian Li, Cheng-Ping Huang, Yan-Feng Chen, Yong-Yuan Zhu, Shi-Ning Zhu, and Nai-Ben Ming. 2007. "Extraordinary Acoustic Transmission Through a 1D Grating with Very Narrow Apertures." *Physical Review Letters* 99 (17): Article ID 174301.

Lu, Zhimiao, Lorenzo Sanchis, Jihong Wen, Li Cai, Yafeng Bi, and José Sánchez-Dehesa. 2018. "Acoustic Cloak Based on Bézier Scatterers." *Scientific Reports* 8 (1): 1–10.

Ma, Guancong, Min Yang, Songwen Xiao, Zhiyu Yang, and Ping Sheng. 2014. "Acoustic Metasurface with Hybrid Resonances." *Nature Materials* 13 (9): 873–878. doi:10.1038/nmat3994.

Mei, Jun, and Ying Wu. 2014. "Controllable Transmission and Total Reflection Through An Impedance-Matched Acoustic Metasurface." *New Journal of Physics* 16 (12): Article ID 123007.

Ni, Xingjie, Naresh K. Emani, Alexander V. Kildishev, Alexandra Boltasseva, and Vladimir M. Shalaev. 2012. "Broadband Light Bending with Plasmonic Nanoantennas." *Science* 335 (6067): 427–427.

Ni, Xingjie, Zi Jing Wong, Michael Mrejen, Yuan Wang, and Xiang Zhang. 2015. "An Ultrathin Invisibility Skin Cloak for Visible Light." *Science* 349 (6254): 1310–1314.

Orazbayev, B., N. Mohammadi Estakhri, M. Beruete, and Andrea Alù. 2015. "Terahertz Carpet Cloak Based on a Ring Resonator Metasurface." *Physical Review B* 91 (19): Article ID 195444.

Pendry, John Brian. 2000. "Negative Refraction Makes a Perfect Lens." *Physical Review Letters* 85 (18): Article ID 3966.

Schurig, David, J. J. Mock, B. J. Justice, Steven A. Cummer, John B. Pendry, A. F. Starr, and David R. Smith. 2006. "Metamaterial Electromagnetic Cloak At Microwave Frequencies." *Science* 314 (5801): 977–980.

Shelby, Richard A., David R. Smith, and Seldon Schultz. 2001. "Experimental Verification of a Negative Index of Refraction." *Science* 292 (5514): 77–79.

Song, Kyungjun, Jedo Kim, Shin Hur, Jun-Hyuk Kwak, Seong-Hyun Lee, and Taesung Kim. 2016. "Directional Reflective Surface Formed Via Gradient-Impeding Acoustic Meta-Surfaces." *Scientific Reports* 6: Article ID 32300.

Tang, Kun, Chunyin Qiu, Manzhu Ke, Jiuyang Lu, Yangtao Ye, and Zhengyou Liu. 2014. "Anomalous Refraction of Airborne Sound Through Ultrathin Metasurfaces." *Scientific Reports* 4: Article ID 6517.

Thomas, T. D., E. Kukk, K. Ueda, T. Ouchi, K. Sakai, T. X. Carroll, C. Nicolas, O. Travnikova, and C. Miron. 2011. “Experimental Observation of Rotational Doppler Broadening in a Molecular System.” *Physical Review Letters* 106 (19): Article ID 193009.

Wang, Hao Gang, Chi Hou Chan, and Kwai-man Luk. 2016. “A Double-Slot Structure as the Metasurface Geometric Phase Generating Atom for Beam Controlling.” In *2016 IEEE International Conference on Computational Electromagnetics (ICCEM)*, 239–241. Piscataway, NY: IEEE. doi:10.1109/COMPEM.2016.7588606.

Yu, Nanfang, Patrice Genevet, Mikhail A. Kats, Francesco Aieta, Jean-Philippe Tetienne, Federico Capasso, and Zeno Gaburro. 2011. “Light Propagation with Phase Discontinuities: Generalized Laws of Reflection and Refraction.” *Science* 334 (6054): 333–337.

Yu, Zhenzhong, Zhong Yang, Yuehong Wang, Haifei Si, and Guoshu Zhao. 2018. “Optimized Cloaks Made of Near-Zero Materials for Different-Sized Concealed Targets.” *Scientific Reports* 8 (1): 1–11.

Zhai, Shilong, Huaijun Chen, Changlin Ding, Linlin Li, Fangliang Shen, Chunrong Luo, and Xiaopeng Zhao. 2016. “Ultrathin Skin Cloaks with Metasurfaces for Audible Sound.” *Journal of Physics D: Applied Physics* 49 (22): Article ID 225302. https://iopscience.iop.org/article/10.1088/0022-3727/49/22/225302/meta.

Zhang, Jing, Zhong Lei Mei, Wan Ru Zhang, Fan Yang, and Tie Jun Cui. 2013. “An Ultrathin Directional Carpet Cloak Based on Generalized Snell’s Law.” *Applied Physics Letters* 103 (15): Article ID 151115.

Zhu, Yi-Fan, Xin-Ye Zou, Bin Liang, and Jian-Chun Cheng. 2015a. “Acoustic One-Way Open Tunnel by Using Metasurface.” *Applied Physics Letters* 107 (11): Article ID 113501.

Zhu, Yi-Fan, Xin-Ye Zou, Bin Liang, and Jian-Chun Cheng. 2015b. “Broadband Unidirectional Transmission of Sound in Unblocked Channel.” *Applied Physics Letters* 106 (17): Article ID 173508.

Zigoneanu, Lucian, Bogdan-Ioan Popa, and Steven A. Cummer. 2014. “Three-Dimensional Broadband Omnidirectional Acoustic Ground Cloak.” *Nature Materials* 13 (4): 352–355. doi:10.1038/nmat3901.